NASA TECHNICAL MEMORANDUM

NASA TM X-1933

NASA TM X-1933

CASE FILE COPY

EFFECT OF A GAS-SOLID SUSPENSION WORKING FLUID ON RADIATOR CHARACTERISTICS FOR A 1-MEGAWATT BRAYTON SPACE POWER CYCLE

by Robert Pfeffer, Salvatore Rossetti, and Seymour Lieblein

Lewis Research Center
Cleveland, Ohio

NATIONAL AERONAUTICS AND SPACE ADMINISTRATION • WASHINGTON, D. C. • DECEMBER 1969

1. Report No. NASA TM X-1933	2. Government Accession No.	3. Recipient's Catalog No.
4. Title and Subtitle EFFECT OF A GAS-SOLID SUSPENSION WORKING FLUID ON RADIATOR CHARACTERISTICS FOR A 1-MEGAWATT BRAYTON SPACE POWER CYCLE		5. Report Date December 1969 6. Performing Organization Code
7. Author(s) Robert Pfeffer, Salvatore Rossetti, and Seymour Lieblein		8. Performing Organization Report No. E-4951
9. Performing Organization Name and Address Lewis Research Center National Aeronautics and Space Administration Cleveland, Ohio 44135		10. Work Unit No. 120-27 11. Contract or Grant No. 13. Type of Report and Period Covered
12. Sponsoring Agency Name and Address National Aeronautics and Space Administration Washington, D.C. 20546		Technical Memorandum 14. Sponsoring Agency Code
15. Supplementary Notes		

16. Abstract

Radiator heat-transfer and geometric characteristics were calculated for a high-temperature 1-megawatt single-loop Brayton space power cycle containing inert-gas graphite-suspension working fluids. For optimum conditions, particle radiation had a relatively small effect on overall heat transfer, and resulted in only a 2 to 3 percent reduction in minimum radiator planform area. Maximum reduction in minimum planform area with a suspension varied from 9 percent for argon to 13 percent for helium.

17. Key Words (Suggested by Author(s))	18. Distribution Statement
Brayton cycle Radiator Gas-solid suspension	Unclassified - Unlimited

19. Security Classif. (of this report)	20. Security Classif. (of this page)	21. No. of Pages	22. Price*
Unclassified	Unclassified	31	$3.00

*For sale by the Clearinghouse for Federal Scientific and Technical Information
Springfield, Virginia 22151

EFFECT OF A GAS-SOLID SUSPENSION WORKING FLUID ON RADIATOR CHARACTERISTICS FOR A 1-MEGAWATT BRAYTON SPACE POWER CYCLE

by Robert Pfeffer,* Salvatore Rossetti,† and Seymour Lieblein

Lewis Research Center

SUMMARY

An analysis has been conducted of the radiator heat-transfer and geometric characteristics of a high-temperature 1-megawatt single-loop Brayton space power cycle containing inert-gas graphite-suspension working fluids. The analysis considered helium, neon, and argon with inclusion of internal radiation heat transfer from the suspension particles. Cycle temperature ratios and particle loading ratios for minimum radiator planform area were determined for a tube-flow Reynolds number of 50 000.

For optimum conditions (minimum planform area), particle radiation had a relatively small effect on overall heat transfer, and resulted in only a 2 to 3 percent reduction in minimum radiator planform area. Maximum indicated reduction in minimum planform area compared with the pure gas case ranged from 9 percent for the argon suspension to 13 percent for the helium suspension for the range of variables and cycle conditions covered. Considerably larger relative variations were found for tube number, length, and internal diameter and for panel aspect ratio. Tube and panel geometry also varied substantially with the gas used.

The overall reduction in planform area resulting from the use of the gas-solid suspension varied with the magnitude of the cycle component efficiencies. For identical component efficiencies, the planform area reduction calculated for the high-temperature 1-megawatt cycle was nearly the same as that for a comparable low-temperature 100-kilowatt cycle analyzed in an earlier study.

---

* Associate professor, City College of City University of New York.

† Graduate student, City College of City University of New York.

INTRODUCTION

Advanced space power generation systems must be able to continuously supply electrical power for long periods of time. One such power generating system currently under technical evaluation is the indirect-conversion closed-loop heat engine based on the Brayton cycle. In this system, heat is generated in a nuclear or solar source and rejected by a radiator, with power being obtained from a turbine located in the working fluid cycle.

Several analyses of potential performance of a Brayton cycle using an inert gas as the working fluid have been conducted (refs. 1 to 4). These studies have indicated that, due to the relatively low temperature levels in the radiator and the inherently low heat-transfer coefficients of gases, the Brayton-cycle waste-heat rejection structure in a single-loop system is relatively large and heavy.

One method that has been proposed to decrease the radiator area and, hence, its weight in a single-loop system is the use of a gas-solid suspension rather than a pure gas as the cycle working fluid. The effect of using a gas-solid suspension as the working fluid on the radiator characteristics of a 100-kilowatt Brayton space power generation system has shown (ref. 5) that the addition of graphite particles to an inert gas working fluid can result in a reduction of approximately 10 to 20 percent in the required minimum radiator planform area.

As the design power level of the Brayton cycle powerplant is increased, the average temperature in the radiator generally increases. Therefore, at high power levels, direct radiation from the solid particles to the tube wall (which was neglected for the 100-kilowatt system studied in ref. 5) might conceivably increase the overall heat transfer to the wall and thus further lower the required radiator planform area.

This study determines the overall effect of gas-solid suspensions and particle radiation on the geometric characteristics of the radiator of a 1-megawatt Brayton space power cycle. The analysis is based on a radiator model identical to that used in reference 5, but with the addition of particle radiation to the tube wall in the heat-transfer relations. The effect of particle loading ratio on the convection and radiation heat-transfer coefficients and on the radiator planform area and panel tube geometry is also presented.

ANALYSIS

Geometrically, the radiator can be identified by its planform area A_{pl}, tube inside diameter D_i, tube length L, number of tubes N, and panel aspect ratio φ (symbols are defined in appendix A). These radiator geometric characteristics are largely determined by the thermodynamics of the power cycle and the heat-transfer and pressure drop capabilities of the working fluid. The governing equations that are required in calculating the

effect of various gas-solid suspension working fluids on these geometric characteristics of the radiator are presented herein. The procedure used in developing these relations is basically the same as that described in detail in reference 5.

Power Cycle

A schematic flow diagram of a single-loop Brayton cycle is shown in figure 1. The numbers correspond to the state-point designations used in this analysis. The gas leaving the heat source at point 1 expands through the turbine to point 2 thereby producing the mechanical work necessary to drive the compressor and alternator. From the turbine the gas enters the recuperator where it is cooled to point 3, as it transfers heat to the gas leaving the compressor. Final cooling to point 4 takes place in the radiator where the excess heat is rejected to space. The gas leaving the radiator is then compressed to point 5, heated in the recuperator to point 6, and further heated back to point 1 in the heat source.

In general, a power cycle analysis provides equations that enable the determination of the working fluid flow rate W, the prime radiating area A_p, and the radiator terminal temperatures T_3 and T_4 from overall cycle parameters and component performance inputs. Prime radiating area A_p is defined as the area of either a tubular radiator without fins or a tube-and-fin radiator with 100 percent efficiency. Equations for these quantities for the Brayton cycle shown in figure 1 have already been developed in refer-

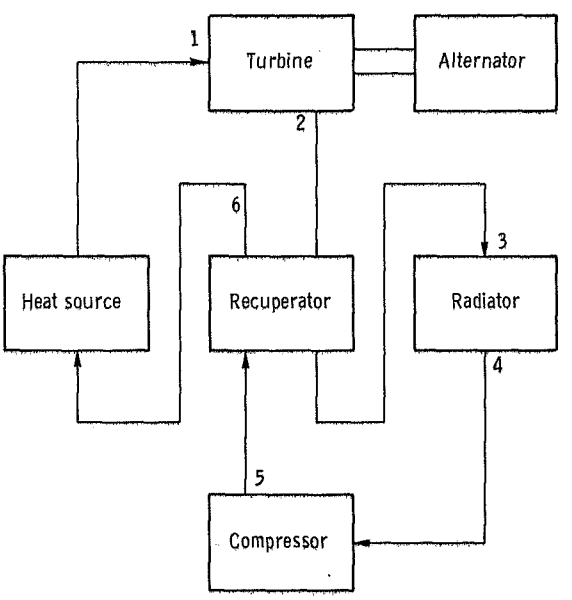

Figure 1. - Flow diagram of single-loop Brayton cycle. (Numbers are state-point designations.)

ences 1 and 5 for the case of no particle radiation heat transfer. However, in this study suspension particle radiation to the tube inside walls will be included in addition to heat convection.

When solid particles are present in a flowing gaseous stream which is at a higher temperature than the surrounding wall, heat will be transferred to the wall by radiation from the particles in addition to heat transfer by convection from the suspension. (It is assumed that heat conduction through the tube walls has a negligible effect on the radiator external temperatures.) The radiant heat flux to the wall due to the particle laden flow will depend on the gas and wall temperatures and on overall view factor or radiation efficiency $\mathcal{F}$, defined as the ratio of the actual radiation emitted by the suspension compared with the maximum radiative energy that can be emitted.

Thus, for an element of tube length, the heat transferred from the gas-solid suspension by both convection and radiation to the tube wall must equal the heat radiated to outer space, so that

$$h_i\left(T_s - T_w\right)dA_i + \mathcal{F}\sigma\left(T_s^4 - T_w^4\right)dA_i = \sigma\epsilon\left(T_w^4 - T_{sp}^4\right)dA_p \tag{1}$$

The determination of the value for $\mathcal{F}$ is discussed in appendix B.

The convection heat-transfer coefficient h_R based on prime radiating area A_p is defined as

$$h_R = h_i \frac{dA_i}{dA_p} \tag{2}$$

where for a suspension

$$h_i = h_s$$

Similarly, the radiation heat-transfer coefficient h_q based on prime radiating area A_p is defined as

$$h_q = \mathcal{F}\sigma \frac{dA_i}{dA_p} \tag{3}$$

Substitution of equations (2) and (3) into equation (1) yields

$$h_R\left(T_s - T_w\right) + h_q\left(T_s^4 - T_w^4\right) = \sigma\epsilon\left(T_w^4 - T_{sp}^4\right) \tag{4}$$

Equation (4) relates the wall temperature T_w to the suspension bulk temperature

T_s at any point along the radiator. For a given radiator outlet temperature T_4, the standard cycle analysis (ref. 1) determines the radiator inlet temperature T_3. The radiator temperature drop $(T_3 - T_4)$ can then be arbitrarily divided into small segments and the wall temperature at each of these segments can be determined by solving equation (4) numerically. Once the wall temperatures have been determined, the prime radiating area A_p can be determined from the following heat balance around an element of radiator tube length:

$$-W_s\left(C_p\right)_s dT_s = \sigma\epsilon\left(T_w^4 - T_{sp}^4\right)dA_p \tag{5}$$

so that

$$A_p = -\frac{W_s\left(C_p\right)_s}{\sigma\epsilon}\int_{T_{w,3}}^{T_{w,4}} \frac{dT_s}{T_w^4 - T_{sp}^4} \tag{6}$$

Equation (6) can be integrated numerically along the points where the wall temperature has been computed between the inlet and outlet temperatures of the radiator.

Gas-Solid Suspension

The gas-solid suspension characteristics required in this analysis were taken mostly from the relations presented in reference 6. Some of the more important of these relations are summarized in the following paragraphs.

Specific heat and its ratios. - The specific heat C_p of a gas is a unique value for that gas. However, for a gas-solid suspension, the value of the specific heat will depend on the specific heats of the carrier gas and the particle and on the particle loading ratio η defined as the ratio of the mass flow rate of solid particles to that of the pure gas,

$$\eta = \frac{W_p}{W_g} \tag{7}$$

The specific heat of the suspension is given by

$$\left(C_p\right)_s = \left(C_p\right)_g\left(\frac{1 + \delta\eta}{1 + \eta}\right) \tag{8}$$

where δ is defined as the ratio of specific heat of the particles to that of the pure gas

$$\delta = \frac{(c_p)_p}{(c_p)_g} \tag{9}$$

The proper value to be used for the isentropic heat ratio of a suspension γ_s is not as clearly defined as for the specific heat. If, however, equilibrium between gas and particles can be assumed ($T_p = T_g$, $V_p = V_g$), the isentropic specific heat ratio of a suspension γ_s in terms of the readily available properties of the system can be estimated by (ref. 6)

$$\gamma_s = \gamma_g \left(\frac{1 + \delta\eta}{1 + \gamma_g \delta\eta} \right) \tag{10}$$

For a suspension, the specific heat ratio will be less than that of the carrier gas. For large loading ratios $\eta > 10$, $\gamma_s \to 1.0$, and the suspension behavior approaches that of an incompressible fluid.

Friction factor. - The friction factor ratio f'_s/f_g is assumed to be adequately represented by the relation given in reference 6

$$\frac{f'_s}{f_g} = 1 + 4.0(Re)_g^{-0.32}\,\eta \tag{11}$$

For fully developed turbulent flow in smooth pipes

$$f_g = 0.046(Re)_g^{-0.2} \tag{12}$$

Convective heat transfer. - The convective heat-transfer coefficient ratio h_s/h_g based on tube inside area A_i is given by (ref. 6)

$$\frac{h_s}{h_g} = 1 + 4.0(Re)_g^{-0.32}\,\delta\eta \tag{13}$$

For turbulent flow

$$h_g = 0.023 \frac{k_g}{D_i} (Re)_g^{0.8} (Pr)_g^{0.3}$$

or

$$h_g = 0.023 \frac{k_g}{D_i} (Re)_g^{0.8} \left[\frac{(C_p)_g \mu_g}{k_g} \right]^{0.3} \tag{14}$$

Suspension radiative heat transfer. - The suspension radiation efficiency in equation (1) is determined from the equation (appendix B)

$$\frac{1}{\mathcal{F}} = \frac{3}{16} \tau + \frac{1}{\epsilon_w} - \frac{1}{2} + \frac{9}{8\tau} \tag{15}$$

where the optical thickness τ is approximated by the relation

$$\tau = \frac{3}{2} \eta \frac{\rho_g}{\rho_p} \frac{D_i}{D_p} \tag{16}$$

In order to compare the effect of suspension radiation heat transfer with that of the convection heat transfer, a pseudo-radiation heat-transfer coefficient h_Q is defined as

$$h_Q = h_q \frac{(T_s^4 - T_w^4)}{(T_s - T_w)} \tag{17}$$

Since T_s and T_w vary along the radiator tube, an average value of h_Q was determined by applying equation (17) to a number of equally spaced points along the tube and averaging the values obtained. The relative magnitude of the effect of radiation from the particles to the tube wall compared with the total heat-transfer rate to the tubes is indicated by the quantity ψ defined as

$$\psi = \frac{h_Q}{h_R + h_Q} \tag{18}$$

Radiator Geometry

The radiator configuration considered in the analysis is identical to that presented in reference 5 and consists of a central fin-tube panel geometry of axial length L and N number of tubes as indicated in figure 2. The tubes are of inside diameter D_i and outside diameter D_o, and the rectangular fins are of thickness t_f and width $2l_f$. Heat rejection occurs from the outside surface of the tubes and from both surfaces of the fins by radiation to space. For simplicity, the headers are neglected, and only the fin-tube panel

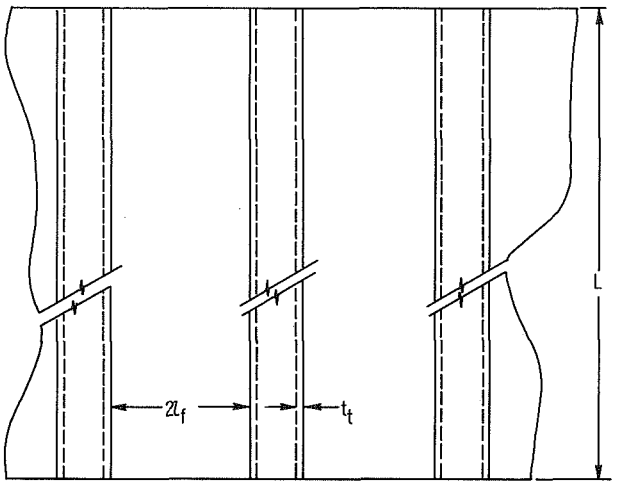

(a) Plan view.

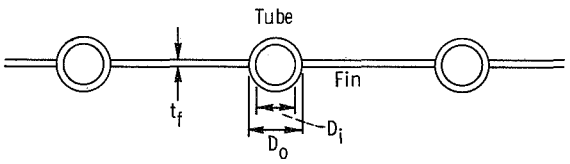

(b) Cross sectional view.

Figure 2. - Central fin-tube radiator configuration.

is considered. In addition, representative constant values of l_f/D_o, η_f, and D_o/D_i are chosen for all cycle conditions as was done in reference 5. Based on this simplified model geometry and these assumptions, equations determining the radiator pressure relations and radiator panel geometry were developed in reference 5. The principal equations will be repeated in the following paragraphs.

Heat-transfer coefficient. - The cycle calculation requires a value of convective heat-transfer coefficient h_R, based on prime radiating area A_p, given by equation (2). In terms of the radiator model of figure 2, the prime and inside areas A_p and A_i of equation (2) are, respectively,

$$A_p = 2D_i\left(\frac{D_o}{D_i}\right)\left[1 + 2\eta_f \frac{l_f}{D_o} LN\right] \tag{19}$$

and

$$A_i = \pi D_i LN \tag{20}$$

Thus, the convective heat-transfer coefficient h_R is (from eqs. (2), (19), and (20))

$$h_R = \frac{h_i}{\left(\frac{D_o}{D_i}\right)\frac{2}{\pi}\left[1 + 2\eta_f\left(\frac{l_f}{D_o}\right)\right]} \tag{21}$$

For a suspension $h_i = h_s$, where h_s is obtained from equations (13) and (14).

Tube geometry. - The tube inside diameter D_i is obtained from the relation for friction pressure drop (ref. 5) based on equations (11) and (12), and the relation for gas-flow Reynolds number given by

$$(Re)_g = \frac{W_s}{\mu_g(1 + \eta)\frac{\pi}{4} D_i N} \tag{22}$$

so that

$$D_i = \sqrt[3]{0.092 \frac{(Re)_g^{1.8}}{(\Delta P)_{rad}}\left[1 + 4.0(Re)_g^{-0.32}\eta\right]\left(\frac{LF\mu^2 R' T_3}{g_c P_3}\right)} \tag{23}$$

where

$$F = 1.5\left[\frac{1 - \left(\frac{T_3}{T_4}\right)^2}{1 - \left(\frac{T_3}{T_4}\right)^3}\right] \tag{24}$$

and

$$P_3 = P_2 - \left(\frac{K_2}{1 - K_2}\right)(\Delta P)_{rad} \tag{25}$$

In equation (25), K_2 is defined as the ratio of the pressure drop in the cold side of the recuperator to the total pressure drop in the cold side of the cycle (radiator and recuperator), or

$$K_2 \equiv \frac{(\Delta P)_{rec}}{(\Delta P)_c} \tag{26}$$

Furthermore, the value of P_2 is obtained from the turbine pressure ratio given by

$$\frac{P_1}{P_2} = \left[1 - \frac{1}{\eta_T}\left(1 - \frac{T_2}{T_1}\right)\right]^{-(\gamma_s/\gamma_s - 1)} \tag{27}$$

For equations (23) and (25), the pressure drop across the radiator $(\Delta P)_{rad}$ is obtained in terms of the cycle loss pressure ratio from

$$(\Delta P)_{rad} = \frac{\left(1 - \frac{r_T}{r_C}\right)(1 - K_2)P_1}{\frac{r_T}{r_C}\left(\frac{1 - K_2 - K_1}{K_1}\right) + \frac{P_1}{P_2}} \tag{28}$$

where K_1 is defined as the ratio of the pressure drop in the radiator to the total system pressure drop, or

$$K_1 \equiv \frac{(\Delta P)_{rad}}{(\Delta P)_{tot}} \tag{29}$$

The tube outer diameter D_o is then

$$D_o = D_i\left(\frac{D_o}{D_i}\right) \tag{30}$$

and the tube length L is obtained from equations (19) and (22) as

$$L = \frac{A_p(Re)_g \mu_g \pi(1 + \eta)}{8W_s\left(1 + 2\eta_f \frac{l_f}{D_o}\right)\left(\frac{D_o}{D_i}\right)} \tag{31}$$

Panel geometry. - The number of tubes in the panel N is obtained from equation (22) as

$$N = \frac{4W_s}{\pi \mu_g (Re)_g D_i (1 + \eta)} \tag{32}$$

and the fin length l_f is

$$l_f = D_o\left(\frac{l_f}{D_o}\right) \tag{33}$$

The planform area of the radiator A_{pl} is defined as the projected area of the radiator panel

$$A_{pl} = NLD_o\left(1 + 2\frac{l_f}{D_o}\right) \tag{34}$$

The panel aspect ratio φ is defined as the ratio of overall width to length of the radiator, or

$$\varphi = \frac{L}{N(D_o + 2l_f)} = \frac{L^2}{A_{pl}} \tag{35}$$

CALCULATIONS

Method of Solution

Once the cycle parameters η_T, η_C, E, and r_T/r_C were specified, and the independent variables T_2/T_1, T_4/T_1, P_1, and P_s were chosen, the cycle was fully described for a given pure gas or a specified gas-solid suspension. From the cycle analysis, W and all gas temperatures were determined according to the corresponding equations given in reference 5. Suspension radiation efficiency $\mathcal{F}$ was obtained using equation (15). The wall temperatures along the radiator tubes were computed at 21 equally spaced points by solving equation (4) using the Newton-Raphson technique. Prime radiating areas A_p were obtained by integrating equation (6) numerically using Simpson's method.

By fixing the radiator model constants D_o/D_i, l_f/D_o, η_f, K_1, and K_2 and by prescribing the gas Reynolds number $(Re)_g$ and loading ratio η in the tubes of the radiator, equations (23), (31), (32), (34), and (35) in conjunction with the cycle outputs were used to determine D_i, L, N, A_{pl}, and φ, respectively. An iterative procedure was required based on an initial assumption of D_i because h_R (which is necessary for the cycle analysis) depends on D_i.

The minimum value of the planform area A_{pl} rather than the prime radiating area A_p was selected as the criterion for determining both the optimum cycle temperature ratios and the optimum suspension loading ratio η for each gas. The planform area was

considered to be more representative of radiator size and weight than prime area. Optimum temperature ratios were determined from a scanning of the computer outputs for each value of η.

Inputs

The example chosen for the parametric analysis was a 1-megawatt shaft-power output cycle with a suspension of graphite in either pure helium, neon, or argon as the working fluid. From turbomachinery considerations, compatible values of $T_1 = 3000^{\circ}$ R (1667 K) and $P_1 = 5.8752 \times 10^4$ pounds per square foot (2.813 MN/m^2) were chosen as the turbine entering temperature and pressure, respectively. Values of the compressor, turbine, and recuperator efficiencies were taken as 0.83, 0.89, and 0.80, respectively, for both the pure gases and the gas-solid suspensions. The independent cycle parameters are T_2/T_1, T_4/T_1, and the loss pressure ratio r_T/r_C. In this analysis, T_2/T_1 was varied between 0.70 and 0.95, and T_4/T_1 was varied between 0.25 and 0.50, both in increments of 0.025. All the calculations were conducted at $r_T/r_C = 0.90$, $K_1 = 0.5$, and $K_2 = 0.25$.

The properties of the inert gases (helium, neon, and argon) required as inputs to the analysis were the thermal conductivity k_g, the viscosity μ_g, the specific heat $(C_p)_g$, the isentropic specific heat ratio γ_g, and the gas constant R'. Values of these properties for the temperature range of interest are presented in appendix C. The gas-solid suspensions studied were suspensions of 30-micrometer-diameter graphite particles in these same inert gases. The pertinent physical properties of graphite are also presented in appendix C. Loading ratios η were varied from 0 to 7 in increments of 1 for helium-graphite, from 0 to 3 in increments of 0.5 for neon-graphite, and from 0 to 1.5 in increments of 0.25 for argon-graphite.

Based on previous analyses of gas cycle radiators, representative geometric parameter values were selected as $D_o/D_i = 1.33$, $l_f/D_o = 3.5$, and $\eta_f = 0.67$. For simplicity, a single gas Reynolds number of 50 000 was selected for the calculations. The equivalent sink temperature of the radiator T_{sp} was chosen as 400° R (222 K), and a value of 0.86 was chosen for the emissivity ϵ of both the inner and outer surfaces of the tubes and of the fins.

RESULTS AND DISCUSSION

Optimum Temperature Ratios

Table I summarizes the principal calculated results of the analysis for the three sus-

TABLE I. - RADIATOR CHARACTERISTICS FOR 1-MEGAWATT BRAYTON CYCLE WITH PARTICLE-TO-WALL RADIATION

[Optimum values at gas Reynolds number of 50 000.]

Loading ratio, η	Optimum temperature ratios		Radiator planform area, A_{pl}		Convective heat-transfer coefficient, h_R		Pseudoradiation heat-transfer coefficient, h_Q		Tube inside diameter, D_i		Tube length, L		Number of tubes, N	Panel aspect ratio, φ
	Turbine inlet to outlet, T_2/T_1	Compressor inlet to turbine outlet, T_4/T_1	ft^2	m^2	$\frac{Btu}{(ft^2)(^oR)}$	$\frac{W}{(m^2)(K)}$	$\frac{Btu}{(ft^2)(^oR)}$	$\frac{W}{(m^2)(K)}$	ft	m	ft	m		
Helium-graphite														
0	0.775	0.350	2626	244	58.2	330.3	0	0	0.071	0.022	54.4	16.6	63.9	1.13
1	.800	.375	2427	225	53.3	302.4	1.40	7.94	.084	.026	58.5	17.8	46.4	1.41
2	.800	.375	2337	217	42.9	243.4	2.08	11.80	.107	.033	74.8	22.8	27.4	2.39
3	.825	.400	2294	213	42.3	240.0	2.63	14.92	.116	.035	73.7	22.5	25.3	2.37
4	.825	.400	2281	212	35.7	202.6	2.68	15.21	.142	.043	88.5	27.0	17.1	3.43
5	.825	.400	2301	214	30.4	172.5	2.61	14.81	.173	.053	104.7	31.9	12.0	4.75
6	.850	.425	2313	215	33.0	187.3	2.80	15.89	.168	.051	95.8	29.2	13.5	3.97
7	.850	.425	2342	218	28.9	164.0	2.65	15.04	.199	.061	110.0	33.5	10.1	5.17
Neon-graphite														
0	0.775	0.350	2951	274	32.4	183.9	0	0	0.039	0.012	18.9	5.8	373.5	0.121
.5	.825	.375	2653	246	26.1	148.1	1.58	8.97	.054	.016	27.4	8.4	166.9	.284
.75	.825	.400	2626	244	22.5	127.7	2.13	12.09	.068	.021	30.2	9.2	119.9	.347
1.0	.850	.400	2632	245	22.6	128.2	2.31	13.11	.070	.021	33.7	10.3	104.0	.432
1.5	.875	.425	2710	252	21.8	123.7	2.69	15.26	.081	.025	36.9	11.2	85.7	.503
2.0	.875	.425	2799	260	17.3	98.2	2.58	14.64	.110	.034	48.9	14.9	49.0	.855
2.5	.900	.450	2938	273	19.7	111.8	2.72	15.43	.106	.032	46.6	14.2	56.1	.738
3.0	.900	.450	3048	283	16.6	94.2	2.52	14.30	.135	.041	57.6	17.6	37.0	1.09
Argon-graphite														
0	0.775	0.350	3133	291	25.7	145.8	0	0	0.019	0.006	7.55	2.3	2036.0	0.018
.250	.825	.375	2855	265	20.8	118.0	.92	5.22	.026	.008	11.1	3.4	911.8	.043
.375	.850	.400	2850	265	21.0	119.2	1.38	7.83	.028	.009	11.3	3.4	846.5	.045
.500	.850	.400	2853	265	18.0	102.1	1.63	9.25	.034	.010	13.8	4.2	569.2	.067
.750	.875	.425	2937	273	17.5	99.3	2.21	12.54	.039	.012	15.2	4.6	470.3	.079
1.00	.875	.425	3033	282	14.0	79.4	2.37	13.45	.052	.016	20.1	6.1	271.1	.133
1.25	.900	.450	3154	293	16.0	90.8	2.78	15.78	.050	.015	19.0	5.8	311.8	.114
1.50	.900	.450	3259	303	13.6	77.2	2.77	15.72	.063	.019	23.4	7.1	207.2	.168

pensions considered. The temperature ratios across the turbine T_2/T_1 and the ratios of compressor inlet to turbine inlet temperature T_4/T_1 listed in the table are the temperature ratios at each value of loading ratio η which result in a minimum value of the planform area A_{pl}. As indicated previously, these optimum temperature ratios were determined from a scanning of the computer outputs for each value of η.

As can be seen from table I, both optimum temperature ratios increase with increasing particle loading ratio η. The rate of increase is smallest with helium and most pronounced with argon. The increase in the optimum temperature ratios with increasing

loading ratio η is due to the fact that the isentropic specific heat ratio γ_s decreases with loading ratio so that the temperature drops across both the turbine and compressor decrease. The variation of the optimum temperature ratios with loading ratio was the same as that for the 100-kilowatt cycle studied in reference 5.

Radiator outlet temperature T_4 at the loading ratio η for the smallest planform area A_{pl} was 1200° R (667 K) for all gases. Radiator inlet temperature T_3 for this condition was 1770° R (983 K) for helium and neon, and 1735° R (964 K) for argon.

Heat-Transfer Characteristics

Convective heat-transfer coefficient. - The effect of the gas-solid suspension on the convective heat-transfer coefficient h_R based on prime radiating area A_p is illustrated in figure 3. The values of h_R for the suspension decrease with increasing loading ratio

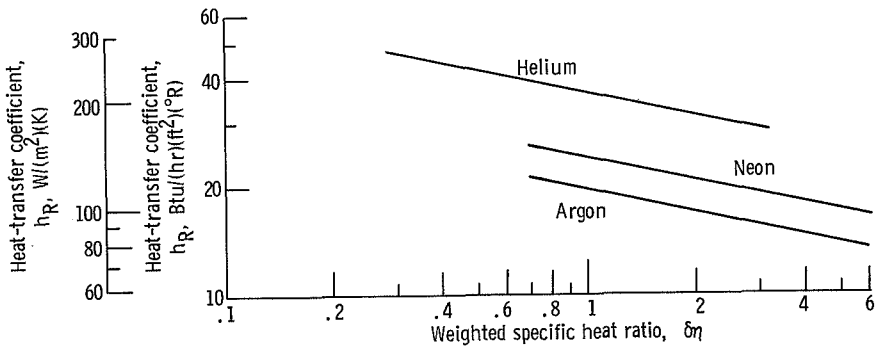

Figure 3. - Variation of convective heat-transfer coefficient with weighted specific heat ratio.

η for all three gases. This apparent anomaly, as discussed in reference 5, is due to the relative variations of h_i for the pure gas and for the suspension. Although the ratio h_s/h_g increases for a given tube diameter D_i as loading ratio η is increased (as indicated by eq. (13)), the tube diameter for the suspension D_i also increases compared with the pure gas case (table I). There is a net decrease in the value of h_s compared with h_g. And with A_i/A_p a constant in all cases (this ratio depends only on geometry), there is a corresponding net reduction in h_R for the suspension as compared with the pure gas case. Figure 3 also shows that the convective heat-transfer coefficient h_R is highest for helium-graphite suspensions and lowest for argon-graphite suspensions.

Radiative heat-transfer coefficient. - The heat transfer by direct radiation between the particles and the tube wall is dependent on the radiation efficiency $\mathcal{F}$ and is also a function of the difference between the suspension bulk temperature and the radiator wall

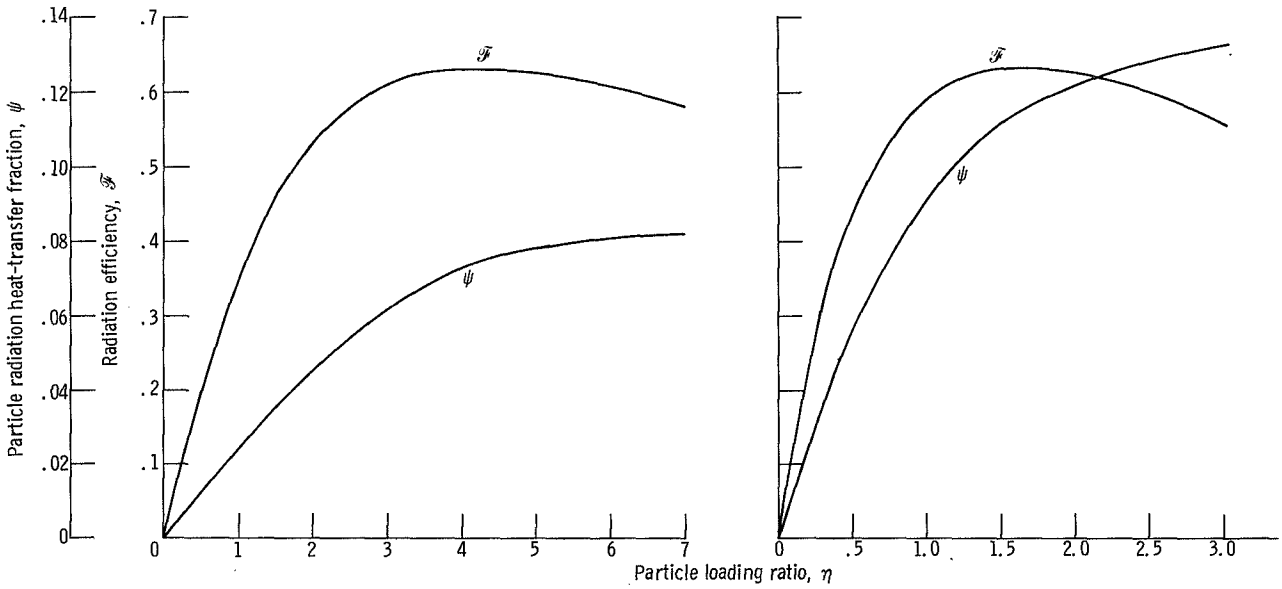

(a) Helium-graphite.

(b) Neon-graphite.

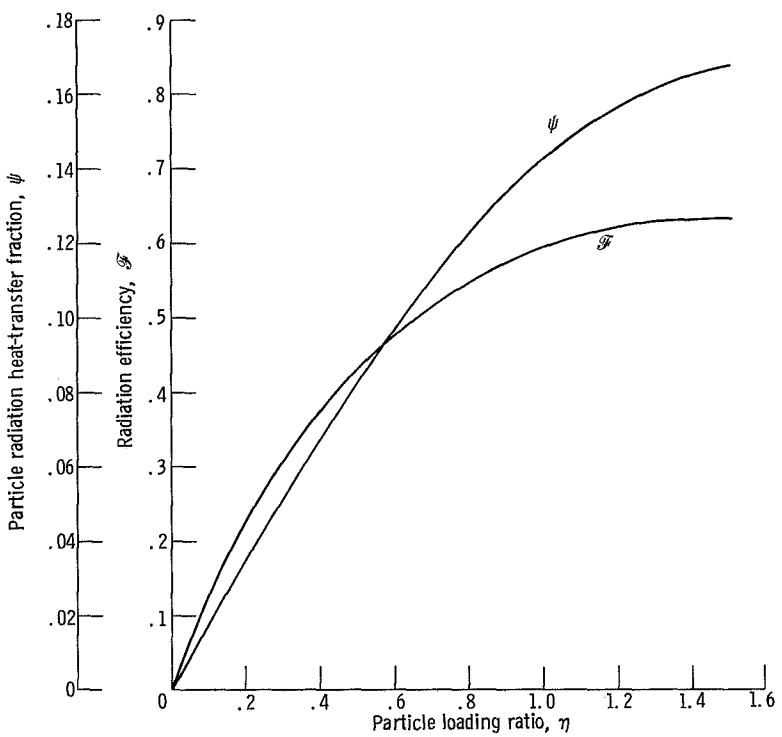

(c) Argon-graphite.

Figure 4. - Variation of particle-to-wall radiation characteristics with particle loading ratio.

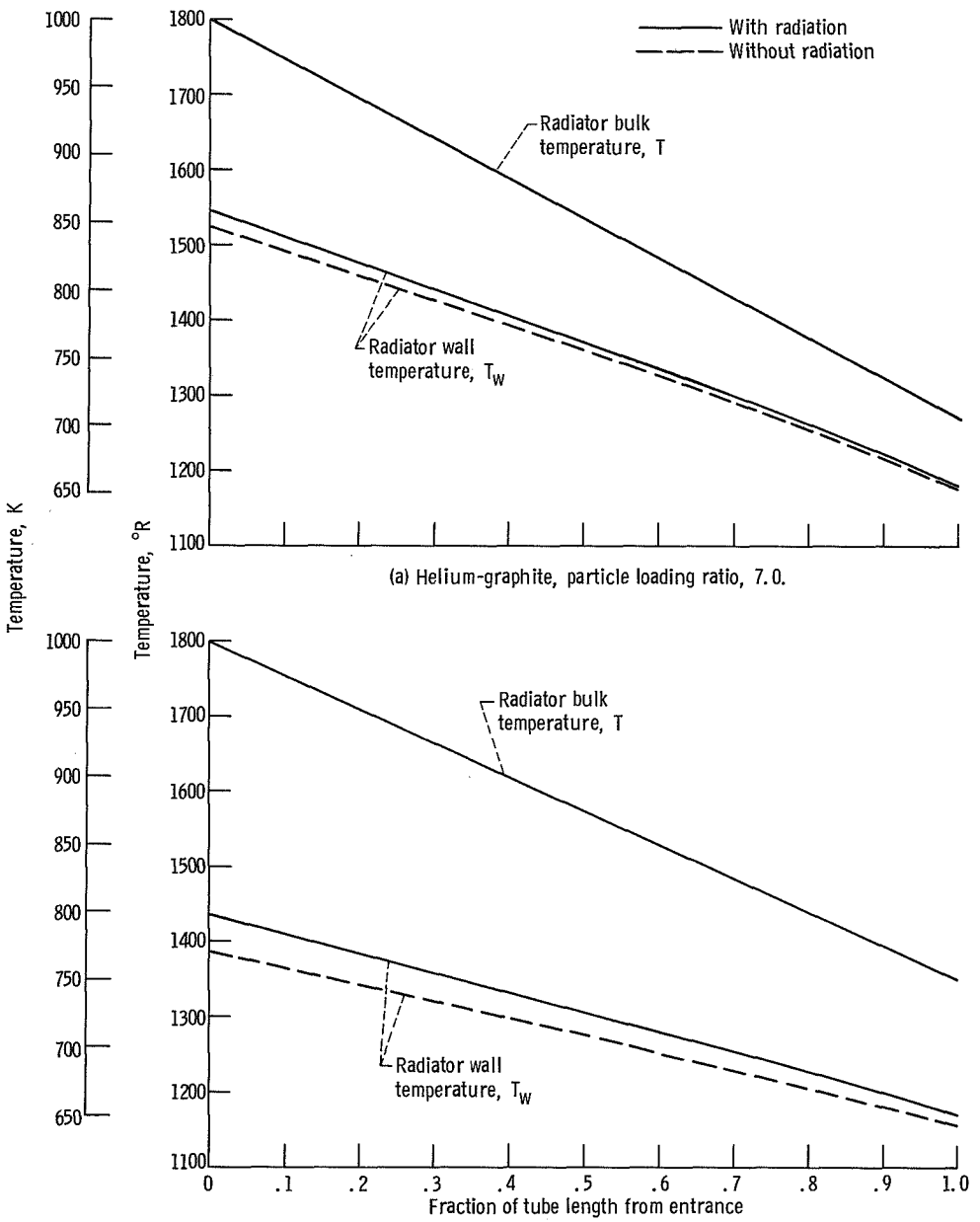

(a) Helium-graphite, particle loading ratio, 7.0.

(b) Argon-graphite; particle loading ratio, 1.5.

Figure 5. - Variation of temperature along tube length.

temperature (eq. (1)). Since the emissivity of the wall ϵ_w is assumed constant at 0.86, $\mathcal{F}$ depends only on the optical thickness τ, which will change with different cycle conditions and particle loadings. Figure 4 shows the variation of radiation efficiency $\mathcal{F}$ with particle loading ratio η for the helium, neon, and argon suspensions using 30-micrometer-diameter graphite particles at optimum cycle conditions (optimum T_2/T_1 and T_4/T_1). For all cases considered, the radiation efficiency $\mathcal{F}$ rises rapidly as particle loading ratio η is increased, reaches a maximum value, and slowly decreases. For the wall emissivity used in this analysis, equation (16) predicts a maximum view factor $\mathcal{F}$ of 0.634. Figure 4 shows that maximum $\mathcal{F}$ is approached at loading ratios η of approximately 4.0, 1.5, and 1.5, respectively, for the helium-, neon-, and argon-graphite suspensions.

Figure 4 also shows the variation of the radiation heat-transfer fraction ψ with loading ratio η. Although $\mathcal{F}$ tends to reach a maximum with loading ratio η, the quantity ψ continues to increase, but at a reduced rate, for the range of loading ratios η covered for each gas. At the maximum values of $\mathcal{F}$ the contribution of the radiation heat transfer to the total heat transfer ψ was around 7.5 percent for helium, 11.5 percent for neon, and 17 percent for argon.

Figure 5 illustrates the effect of particle to wall radiation on the radiator tube wall temperature at the largest values of η considered for the helium-graphite and argon-graphite suspensions. In both cases the difference between the wall temperature, when taking into account particle radiation or when neglecting it, is relatively small, varying from 20° to 50° R (11 to 28 K) at the radiator inlet and from 3° to 15° R (2 to 8 K) at the radiator exit. This small variation in temperature, when compared with the difference in temperature between the wall and the bulk suspension (as also shown in fig. 5), is a reflection of the moderate radiation contribution to the total heat-transfer rate, as already revealed in figure 4.

Radiator Geometry

Tube geometry. - The effect of loading ratio η on such panel geometry characteristics as the length, number, diameter of radiator tubes and radiator panel aspect ratio can be obtained from the values listed in table I. The table shows that, although the planform area A_{pl} decreases to a minimum and then increases as the loading ratio η is increased, the diameter D_i and length L of the radiator tubes continuously increase, whereas the number of radiator tubes N continually decreases in the loading ratio range of interest. The variations in D_i, L, N, and φ were quite pronounced over the range of particle loading ratios covered, with maximum changes in N and φ of around an order of magnitude for the neon and argon suspensions. At minimum planform area, the tube length, inside diameter, and number varied from 50 to 100 percent of the corre-

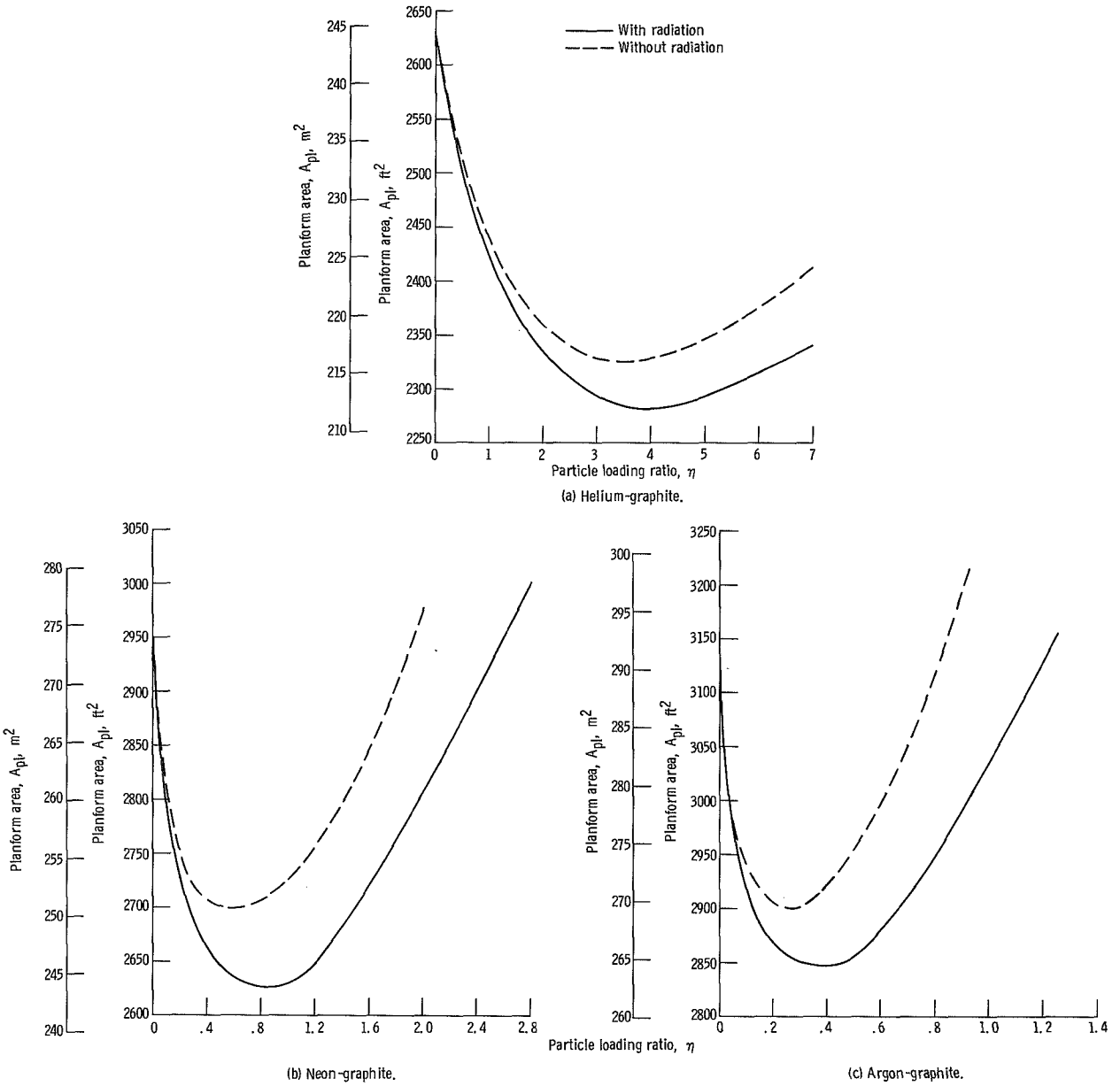

Figure 6. - Variation of radiator planform area with loading ratio.

sponding values for the pure gas, while the panel aspect ratio φ increased by approximately a factor of 3. The use of a solid suspension therefore provides a very effective means for altering the tube and panel geometry at a given gas-flow Reynolds number.

The table also shows that, for a fixed value of gas-flow Reynolds number, the use of helium results in a panel aspect ratio φ approximately 10 times that of neon and 100 times that of argon at minimum A_{pl}. These same trends were observed for the 100-kilowatt cycle studied in reference 5.

Planform area. - The variation of panel planform area A_{pl} with particle suspension loading ratio η including the effect of particle radiation to the wall is shown by the solid curves in figure 6 for the three gases considered. Values of the planform area A_{pl} for $\eta = 0$ represent the pure gas case. The figure shows that a minimum planform area A_{pl} is obtained at a specific loading ratio η for each gas. The optimum loading ratios η are approximately 4.0, 0.85, and 0.375 for the helium-, neon-, and argon-graphite suspensions, respectively. Thus, only for helium do the radiator planform area A_{pl} and radiation efficiency $\mathscr{F}$ optimize at the same value of loading ratio.

The dashed curves plotted in figure 6 represent the planform area A_{pl} as a function of loading ratio neglecting particle-to-wall radiation. Comparing the dashed and solid curves shows that the optimum loading ratio η is slightly higher when the particle radiation is considered but results in only 2 to 3 percent decrease in planform area A_{pl} at the optimum loading ratios η. The decrease in planform area resulting from particle radiation tended to increase for values of η greater than optimum, especially for the neon and argon suspensions. For example, at η for maximum $\mathscr{F}$, the percent reduction in planform area due to particle radiation was 4.5 and 11.0, respectively, for neon and argon.

A minimum of the planform area A_{pl} with loading ratio η is basically due to the opposing effects of the isentropic specific heat ratio γ_s and the convective heat-transfer coefficient h_R. For a given gas, an increase in the solids loading ratio η decreases γ_s, which increases the cycle efficiency and thus tends to decrease the planform area A_{pl}. At the same time, an increase in η decreases h_R (see fig. 3) and, therefore, tends to increase the planform area A_{pl}. The average radiation heat-transfer coefficient h_Q, which is directly related to ψ, increases with loading ratio η for the conditions considered in the analysis (see fig. 4). However, the contribution of h_Q to the tube heat-transfer to the wall is only moderate so that the net effect of h_Q on the optimum loading ratio η is a slight shift in the direction of higher loading ratios as shown in figure 6.

Since γ_s and h_R are both functions of the weighted specific heat ratio $\delta\eta$ this quantity will define the minimum planform area A_{pl}. This is illustrated by figure 7, which shows that for all three graphite-gas suspensions considered the minimum planform area A_{pl} occurs at approximately the same value of $\delta\eta$ equal to 1.3 at the gas Reynolds number of 50 000. Based on the results of figure 7, the magnitude of the de-

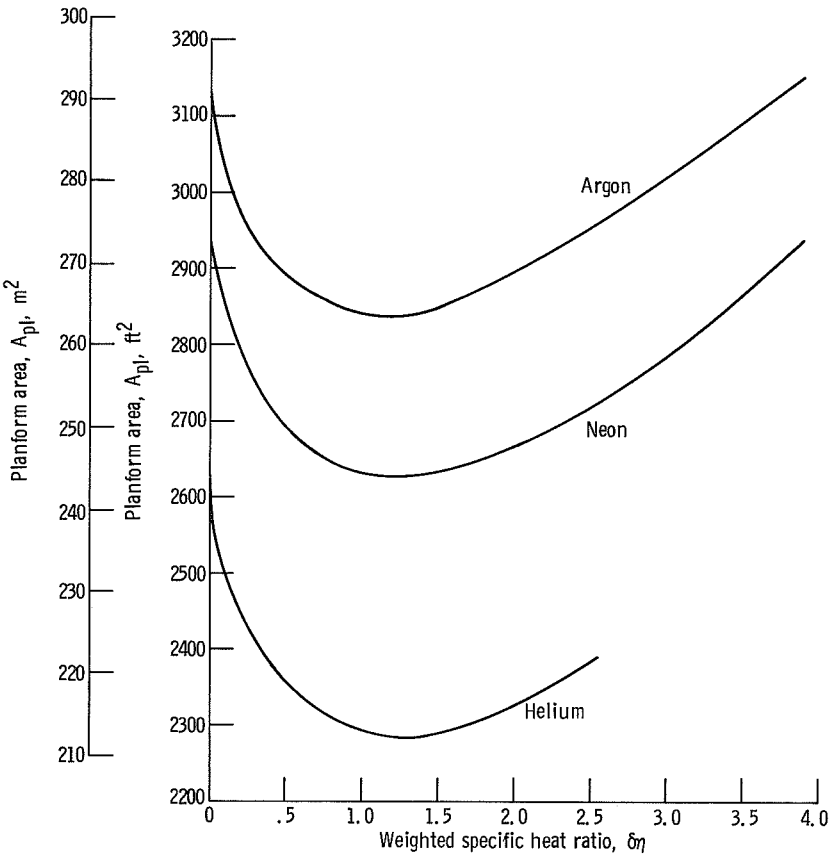

Figure 7. - Variation of radiator planform area with weighted specific heat ratio.

crease in panel planform area obtainable by the use of a graphite-gas suspension in the 1-megawatt Brayton cycle is approximately 13 percent for helium, 11 percent for neon, and 9 percent for argon.

In order to compare the reduction in planform area A_{pl} obtained in the 1-megawatt cycle with the 100-kilowatt cycle studied in reference 5, the ratio of planform area required with a helium-graphite suspension to the planform area required with pure helium was plotted against particle loading ratio η (fig. 8). The upper three curves represent the planform area for the 1-megawatt cycle case with and without consideration of particle radiation in the tube internal heat transfer. The lowest curve is the variation obtained for the 100-kilowatt cycle suspension as reported in reference 5.

It is seen that the percentage reduction in radiator planform area for the 100-kilowatt cycle without consideration of particle radiation was actually greater than the percentage reduction for the 1-megawatt cycle with radiation included. These results were typical of the three suspensions studied. Since the percentage reduction in the convective heat-transfer coefficient h_R was practically the same for both cycles, these results can be explained on the basis of the different values of compressor, turbine, and

recuperator efficiencies used in the two studies. The differences in component efficiencies influenced the effect of the isentropic specific heat ratio γ_s on the overall cycle efficiency and the working fluid mass flow rate W_s, which, in turn, affected the prime area of the radiator A_p to produce a smaller reduction in planform area A_{pl}.

The variation of planform area ratio for the 1-megawatt cycle with particle radiation for the same component efficiency values as for the 100-kilowatt cycle is given by the long-dashed curve. A sizable difference is observed compared with the original results. The relative effect of the use of a suspension working fluid will therefore depend on the magnitude of the component efficiencies selected for the cycle study.

On the basis of the same component efficiencies, figure 8 indicates planform area results that are nearly the same for both cycles considered. Although the calculations of reference 5 did not include the effects of suspension particle radiation, the results obtained can be considered to be very nearly representative of the values if particle radiation had been included. This judgment is based on the observation of the relatively small

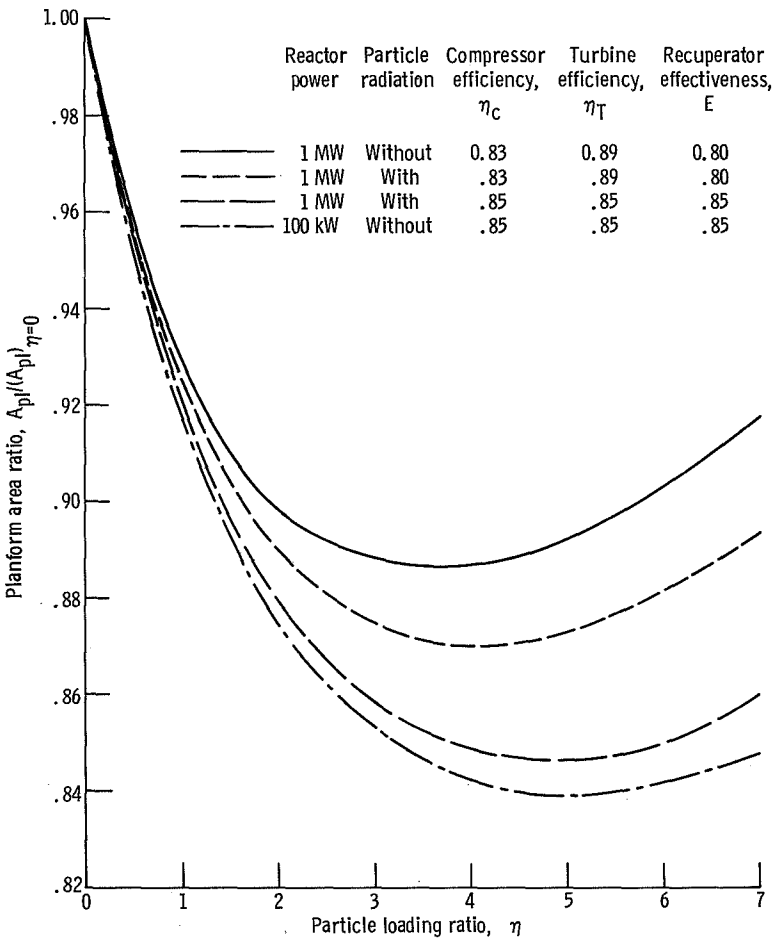

Figure 8. - Effect of cycle condition on ratio of radiator planform area with suspension to planform area with pure gas. Helium-graphite system.

effect of particle radiation on minimum planform area in the high-temperature 1-megawatt case (2 to 3 percent) and the substantially lower cycle temperatures considered for the 100-kilowatt case. Thus, it can be concluded that the planform area reduction results of reference 5 are also representative of the higher power cycle. Maximum reduction in minimum planform area found in the study of reference 5 was around 16 percent for helium.

SUMMARY OF RESULTS

The analysis of the application of an inert gas-graphite suspension with particle radiation as the working fluid in a high-temperature 1-megawatt single-loop Brayton cycle has produced the following major results for optimum cycle temperature ratios and a tube-flow Reynolds number of 50 000:

1. Maximum values of particle-to-wall radiation efficiency $\mathscr{F}$ were attained at particle loading ratios η of approximately 4.0, 1.5, and 1.5, respectively, for the helium, neon, and argon suspensions. At these values of radiation efficiency, particle radiation contributed approximately 7.5, 11.5, and 17 percent, respectively, to the total suspension-to-tube heat transfer. However, the net effect of particle radiation on minimum radiator planform area A_{pl} was relatively small, resulting in only an approximately 2 to 3 percent decrease in radiator planform area compared with the value obtained when particle radiation was neglected.

2. The particle loading ratios η for minimum radiator planform area A_{pl} were 4.0, 0.75, and 0.375, respectively, for the helium, neon, and argon suspensions. The corresponding values of reduction in planform area compared with the pure gas case were about 13 percent for helium, 11 percent for neon, and 9 percent for argon. At minimum planform area A_{pl}, the weighted specific heat ratio $\delta\eta$ was the same at 1.3 for all three gas suspensions.

3. The use of a gas-graphite suspension had a pronounced effect on the number, length, and inside diameter of the tubes and on the panel aspect ratio. Variations of between 50 and 100 percent compared with the pure gas cases were indicated for tube length, diameter, and number at minimum planform area. Panel aspect ratio was increased by a factor of around 3.

4. The magnitude of the reduction in radiator planform area A_{pl} resulting from the use of a gas-solid suspension working fluid varied significantly with the magnitude of the component efficiencies used in the cycle.

5. The calculated radiator characteristics and optimum temperature ratio values were generally similar to those determined for a comparable low-temperature 100-kilowatt cycle analyzed in a previous study. Furthermore, when identical cycle compo-

nent efficiencies were considered, the reduction in radiator planform area A_{pl} for the high-temperature 1-megawatt cycle was nearly the same as for the low-temperature 100-kilowatt cycle.

Lewis Research Center,
National Aeronautics and Space Administration,
Cleveland, Ohio, September 17, 1969,
120-27.

APPENDIX A

SYMBOLS

A	particle cross sectional area, ft^2; m^2
A_i	radiator tube inside surface area, ft^2; m^2
A_p	prime radiating area, ft^2; m^2
A_{pl}	radiator planform area, ft^2; m^2
C_p	fluid heat capacity, Btu/(lbm)(^oR); J/(kg)(K)
D_i	radiator tube inside diameter, ft; m
D_o	radiator tube outside diameter, ft; m
D_p	particle diameter, ft; m
E	recuperator effectiveness
F	correction factor for nonisothermal flow in the radiator
$\mathscr{F}$	radiation efficiency or view factor
f_g	Fanning friction factor for a pure gas
f'_s	friction factor for gas-solid suspension based on gas density, defined by eq. (11)
g_c	gravitational constant, (lbm/lbf) (ft/sec^2); (kg)(m)/(N)(sec^2)
h_i	convective heat-transfer coefficient based on tube inside area, Btu/(ft^2)(^oR)(hr); W/(m^2)(K)
h_Q	pseudoradiation heat-transfer coefficient defined by eq. (17), Btu/(hr)(ft^2)(^oR); W/(m^2)(K)
h_q	radiation heat-transfer coefficient defined by eq. (3), Btu/(hr)(ft^2)(^oR)^4; W/(m^2)(K)^4
h_R	convective heat-transfer coefficient based on radiator prime area, Btu/(ft^2)(^oR)(hr); W/(m^2)(K)
K_1	radiator pressure-drop fraction: ratio of pressure drop through the radiator to total pressure drop in the cycle
K_2	recuperator pressure-drop fraction: ratio of pressure drop through the recuperator to cycle cold side pressure drop
k	absorption coefficient, 1/ft; 1/m
k_g	thermal conductivity of gas, Btu/(sec)(^oR)(ft); J/(sec)(m)(K)
L	length of radiator tubes, ft, m
l_f	half width of fin, ft; m
N	number of radiator tubes
n	number of particles per unit volume of suspension, $1/ft^3$; $1/m^3$
P	gas pressure, lbf/ft^2; N/m^2
Pr	Prandtl number
P_s	output shaft power, kW
$(\Delta P)_c$	sum of pressure drops across radiator and recuperator (cold pressure drop), lbf/ft^2; N/m^2

$(\Delta P)_{rad}$	pressure-drop across the radiator, lbf/ft^2; N/m^2
$(\Delta P)_{rec}$	pressure-drop across cold side of the recuperator, lbf/ft^2; N/m^2
$(\Delta P)_{tot}$	total pressure-drop through heat-transfer components in the cycle, lbf/ft^2; N/m^2
R'	gas constant, (lbf)(ft)/(lbm)(^oR); J/(kg)(K)
$(Re)_g$	gas Reynolds number
r_T/r_C	cycle loss pressure ratio, $(P_1/P_2)/(P_5/P_4)$
T	absolute temperature, ^oR; K
T_{sp}	equivalent sink temperature, ^oR; K
t_f	thickness of fin, ft; m
t_t	thickness of radiator tube, ft; m
V	velocity through radiator tubes, ft/sec; m/sec
W	mass flow rate, lbm/sec; kg/sec
γ	isentropic specific heat ratio
δ	ratio of particle to gas specific heats
ϵ	emissivity
η	loading ratio of suspension, lbm_{solid}/lbm_{gas}; kg_{solid}/kg_{gas}
η_c	compressor efficiency
η_f	fin efficiency
η_T	turbine efficiency
μ	gas viscosity, lbm/(ft)(sec); (N)(sec)/(m^2)
ρ	density, lbm/ft^3; kg/m^3
ρ'_p	bulk density of particles in suspension, lbm/ft^3; kg/m^3
σ	Stefan-Boltzman constant, Btu/(ft^2)($^oR^4$); J/(m^2)(K^4)
τ	optical thickness
φ	radiator panel aspect ratio
ψ	particle-radiation heat-transfer fraction (eq. (18))

Subscripts:

g	gas
p	particle
s	suspension
w	conditions at tube wall
1	turbine inlet
2	turbine outlet
3	radiator inlet
4	radiator outlet
5	compressor outlet
6	heat-source inlet

APPENDIX B

GAS RADIATION EFFICIENCY

The gas radiation efficiency or view factor $\mathscr{F}$ for use in equation (1) was determined from Deissler's diffusion approximation for thermal radiation in gases with jump boundary conditions (ref. 7). For a gray gas flowing through a circular tube of constant diameter, Deissler's results may be approximated by the equation (written in the notation of this report)

$$\frac{1}{\mathscr{F}} = \frac{3}{16}\tau + \frac{1}{\epsilon_w} - \frac{1}{2} + \frac{9}{8\tau} \tag{B1}$$

where τ is the optical thickness of the gas and ϵ_w is the emissivity of the inside wall of the tube.

In general, for an absorbing, nonscattering, gray gas,

$$\tau = kD_i \tag{B2}$$

where k is absorption coefficient and D_i is tube inside diameter. For particle suspensions, k is defined as

$$k = nA \tag{B3}$$

where n is the number of particles in a unit volume of a suspension and A is the average radiation absorption cross section of a single particle in the suspension. For particle sizes greater than the wavelength of the radiation, it can usually be assumed that the absorption cross section of the particle A is equal to its geometric cross section. The particle size considered in this analysis (D_p = 30 μm) is sufficiently large to be treated in this manner.

For spherical particles, the number of particles in a unit volume of suspension n is given by

$$n = \frac{6\rho_p'}{\rho_p \pi D_p^3} \tag{B4}$$

where ρ_p' is the bulk density of the particles ($lbm_{solid}/ft^3_{suspension}$ or $kg_{solid}/m^3_{suspension}$) and ρ_p is the actual density of the particle (lbm_{solid}/ft^3_{solid} or kg_{solid}/m^3_{solid}). However, according to reference 6, the bulk density of the particles ρ_p' may be expressed in terms of the loading ratio η and the density of the carrier gas ρ_g by

$$\rho_p' = \eta \rho_g \tag{B5}$$

Finally, substitution of equations (B3) to (B5) into equation (B2) results in the relation of the optical thickness of a suspension written as

$$\tau = \frac{3}{2} \eta \frac{\rho_g}{\rho_p} \frac{D_i}{D_p} \tag{B6}$$

Equation (B6) together with equation (B1) was used to determine the gas radiation efficiency $\mathscr{F}$ in terms of the inputs considered in this study.

APPENDIX C

PROPERTIES

The values of the gas properties utilized as inputs to the computer program are presented herein. Since both viscosity and thermal conductivity of the gases are dependent on temperature, equations to determine these properties as function of the arithmetic mean temperature in the radiator are given. These equations were obtained from faired curves based on the data of reference 8 in the temperature range from 760° to 1960° R (422 to 1090 K).

Property	U.S. Customary Units	SI Units
	Helium	
C_p	1.25 Btu/(lbm)(°R)	5230 J/(kg)(K)
γ	1.67	1.67
R'	386.25 (lbf/lbm)(ft/°R)	2080 J/(kg)(K)
k_g	$0.0433\ T^{0.650}\times10^{-5}$ Btu/(sec)(ft)(°R)	$0.3950\ T^{0.650}\times10^{-2}$ J/(sec)(m)(K)
μ	$0.0238\ T^{0.650}\times10^{-5}$ lbm/(ft)(sec)	$0.0519\ T^{0.650}\times10^{-5}$ (N)(sec)/m^2
	Neon	
C_p	0.25 Btu/(lbm)(°R)	1046 J/(kg)(K)
γ	1.67	1.67
R'	77.25 (lbf/lbm)(ft/°R)	416 J/(kg)(K)
k_g	$0.0128\ T^{0.662}\times10^{-5}$ Btu/(sec)(ft)(°R)	$0.1176\ T^{0.662}\times10^{-2}$ J/(sec)(m)(K)
μ	$0.0232\ T^{0.665}\times10^{-5}$ lbm/(ft)(sec)	$0.0509\ T^{0.665}\times10^{-5}$ (N)(sec)/m^2
	Argon	
C_p	0.125 Btu/(lbm)(°R)	523 J/(kg)(K)
γ	1.67	1.67
R'	38.63 (lbf/lbm)(ft/°R)	208 J/(kg)(K)
k_g	$0.00298\ T^{0.725}\times10^{-5}$ Btu/(sec)(ft)(°R)	$0.0284\ T^{0.725}\times10^{-2}$ J/(sec)(m)(K)
μ	$0.0156\ T^{0.725}\times10^{-5}$ lbm/(ft)(sec)	$0.0355\ T^{0.725}\times10^{-5}$ (N)(sec)/m^2

The specific heat of graphite over the temperature range 500° to 2000° R (278 to 1112 K) was taken as 0.400 Btu per pound mass per $^{\circ}$R (1674 J/(kg)(K)). Therefore, the values of δ which were used for the suspensions are

Suspension	Particle to gas specific heat ratio, δ
Helium-graphite	0.312
Neon-graphite	1.56
Argon-graphite	3.12

It was also assumed that the average diameter of the graphite particles is 30 micrometers, the density of the graphite particles is 96.5 pounds per cubic foot (1546 kg/m^3), and the absorptivity is 1. An average particle diameter of 30 micrometers was selected to provide for a stable suspension for the range of optimum loading ratios covered. This value should be above that for which surface coating due to Brownian effects might occur (refs. 9 and 10) and below that for which deposition due to overloading and inertial effects might result (refs. 11 and 12).

REFERENCES

1. Glassman, Arthur J.; and Stewart, Warner L.: Thermodynamic Characteristics of Brayton Cycles for Space Power. J. Spacecraft Rockets, vol. 1, no. 1, Jan.-Feb. 1964, pp. 25-31.

2. Stewart, Warner L.; Glassman, Arthur J.; and Krebs, Richard P.: The Brayton Cycle for Space Power. Paper 741A, SAE, Sept. 1963.

3. Glassman, A. J.; Krebs, R. P.; and Fox, T. A.: Brayton Cycle Nuclear Space Power Systems and Their Heat-Transfer Components. Chem. Eng. Progr. Symp. Ser., vol. 61, no. 57, 1965, pp. 306-314.

4. Norman, L. W.: The Application of the Recuperated Brayton Cycle to Space Power Conversion Systems. Paper 63-220, AIAA, June 1963.

5. Pfeffer, Robert; Rossetti, Salvatore; and Lieblein, Seymour: Analysis of Radiator Characteristics of a Single-Loop 100-Kilowatt Brayton Space Power System Using a Pure Gas and a Gas-Solid Suspension. NASA TN D-4659, 1968.

6. Pfeffer, Robert; Rossetti, Salvatore; and Lieblein, Seymour: Analysis and Correlation of Heat-Transfer Coefficient and Friction Factor Data for Dilute Gas-Solid Suspensions. NASA TN D-3603, 1966.

7. Deissler, R. G.: Diffusion Approximation for Thermal Radiation in Gases with Jump Boundary Conditions. J. Heat Transfer, vol. 86, no. 2, May 1964, pp. 240-246.

8. Svehla, Roger A.: Estimated Viscosities and Thermal Conductivities of Gases at High Temperatures. NASA TR R-132, 1962.

9. Schluderberg, Donald C.; Whitelaw, R. L.; and Carlson, Robert W.: Gaseous Suspensions - A New Reactor Coolant. Nucleonics, vol. 19, no. 8, Aug. 1961.

10. Wachtell, G. P.; Waggener, J. P.; and Steigelmann, W. H.: Evaluation of Gas-Graphite Suspensions as Nuclear Reactor Coolants. Rept. No. NYO-9672, AEC, Aug. 1961.

11. Zenz, F. A.: Conveyability of Materials of Mixed Particle Size. I.&E.C. Fundamentals, vol. 3, Feb. 1964, p. 65.

12. Rossetti, Salvatore: The Effect of Particle and Fluid Properties on the Pressure Drop and Heat Transfer Coefficient of Dilute Flowing Gas-Solid Suspension. Doctoral thesis submitted to City College, City University of New York, Aug. 1969.

NASA-Langley, 1969 —— 3 E-4951

NATIONAL AERONAUTICS AND SPACE ADMINISTRATION
WASHINGTON, D. C. 20546

OFFICIAL BUSINESS

FIRST CLASS MAIL

POSTAGE AND FEES PAID
NATIONAL AERONAUTICS AND
SPACE ADMINISTRATION

POSTMASTER: If Undeliverable (Section 158 Postal Manual) Do Not Return

"The aeronautical and space activities of the United States shall be conducted so as to contribute . . . to the expansion of human knowledge of phenomena in the atmosphere and space. The Administration shall provide for the widest practicable and appropriate dissemination of information concerning its activities and the results thereof."

—NATIONAL AERONAUTICS AND SPACE ACT OF 1958

NASA SCIENTIFIC AND TECHNICAL PUBLICATIONS

TECHNICAL REPORTS: Scientific and technical information considered important, complete, and a lasting contribution to existing knowledge.

TECHNICAL NOTES: Information less broad in scope but nevertheless of importance as a contribution to existing knowledge.

TECHNICAL MEMORANDUMS: Information receiving limited distribution because of preliminary data, security classification, or other reasons.

CONTRACTOR REPORTS: Scientific and technical information generated under a NASA contract or grant and considered an important contribution to existing knowledge.

TECHNICAL TRANSLATIONS: Information published in a foreign language considered to merit NASA distribution in English.

SPECIAL PUBLICATIONS: Information derived from or of value to NASA activities. Publications include conference proceedings, monographs, data compilations, handbooks, sourcebooks, and special bibliographies.

TECHNOLOGY UTILIZATION PUBLICATIONS: Information on technology used by NASA that may be of particular interest in commercial and other non-aerospace applications. Publications include Tech Briefs, Technology Utilization Reports and Notes, and Technology Surveys.

Details on the availability of these publications may be obtained from:

SCIENTIFIC AND TECHNICAL INFORMATION DIVISION

NATIONAL AERONAUTICS AND SPACE ADMINISTRATION

Washington, D.C. 20546